

WISSENSCHAFTLICH-TECHNISCHE BERICHTE

FZR-325

Juli 2001

ISSN 1437-322X

Archiv-Ex.:

Mirela Gavrilas und Thomas Höhne

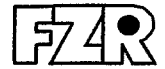
**OECD/CSNI ISP NR. 43 Rapid Boron Dilution
Transient Tests for Code Verification
Post Test Calculation with CFX-4**

Herausgeber:
Forschungszentrum Rossendorf e.V.
Postfach 51 01 19
D-01314 Dresden
Telefon +49 351 26 00
Telefax +49 351 2 69 04 61
<http://www.fz-rossendorf.de/>

Als Manuskript gedruckt
Alle Rechte beim Herausgeber

FORSCHUNGSZENTRUM ROSSENDORF

WISSENSCHAFTLICH-TECHNISCHE BERICHTE



FZR-325

Juli 2001

Mirela Gavrilas und Thomas Höhne

**OECD/CSNI ISP NR. 43 Rapid Boron Dilution
Transient Tests for Code Verification
Post Test Calculation with CFX-4**

OECD/CSNI ISP NR. 43
RAPID BORON DILUTION TRANSIENT TESTS FOR CODE
VERIFICATION
POST TEST CALCULATION WITH CFX-4

Mirela Gavrilas

University of Maryland
Department of Materials and Nuclear Engineering
College Park, MD 20742-2115 / USA

Thomas Höhne

Research Center Rossendorf (FZR)
Institute for Safety Research
D - 01314 Dresden / Germany

Table of Contents

1. The ISP-43 Tests	2
1.1 Test A—single inlet, single outlet, external tank injection.....	3
1.2 Test B—single inlet, single outlet, steam generator injection	4
2. Temperature Measurement	5
3. Computational Modeling.....	10
3.1 Choice of models and nodalization.....	10
3.2 Model assumptions, geometry preparation and grid generation.....	11
4. Results	13
4.1 Test A.....	13
4.2 Test B	18
5. Conclusion.....	25
Literature	25

1. The ISP-43 Tests

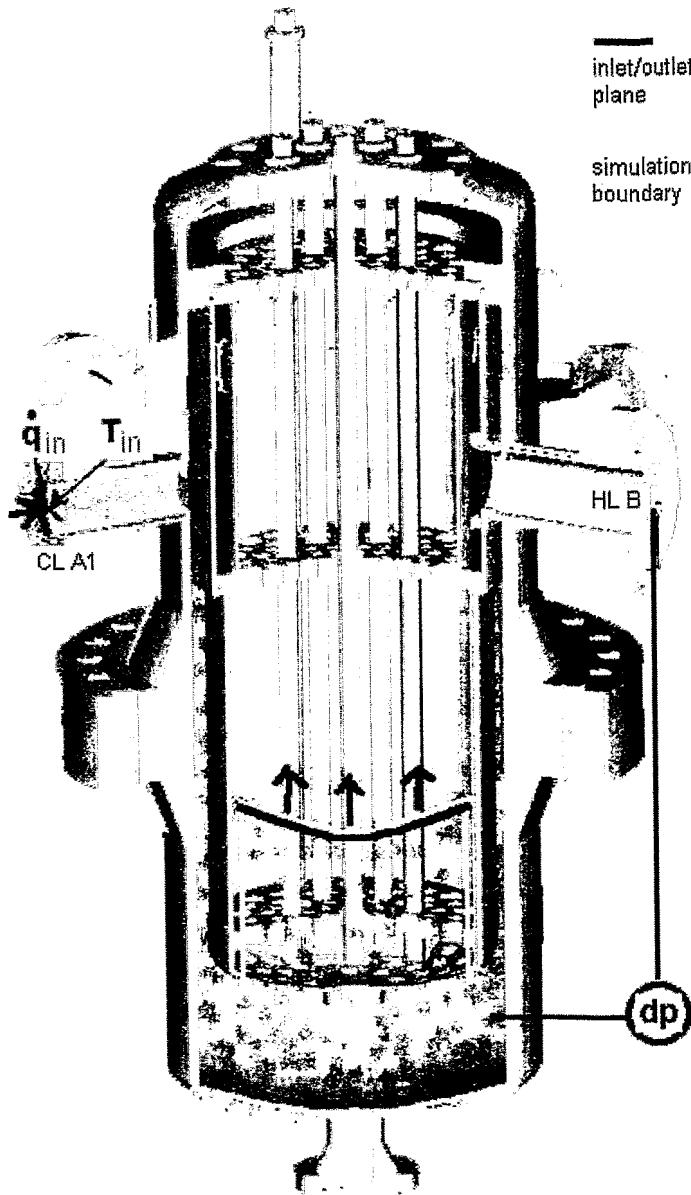


Fig. 1 Boundary Conditions ISP 43

The test series for the International Standard Problem ISP 43 at the University of Maryland provides a platform for experiences gained by research groups to be applied to the simulation of a well-defined test series [Ga]. Ten organizations from eight countries participated in the exercise. All used computational fluid dynamics (CFD) codes to obtain predictions. Most participants used commercial software (Fluent, CFX) while some used independently developed codes (TRIO-U, PLASHY).

The University of Maryland, College Park 2x4 Thermal-Hydraulic Loop Facility is a scaled down model of the Three Mile Island Unit 2 Babcock & Wilcox (B&W) pressurized water reactor (PWR). The main components of the model reactor coolant system (RCS) include a reactor vessel, two hot legs, two once-through steam generators (SGs), four cold legs, four reactor coolant pumps (RCPs), and one pressurizer. Because the UM 2x4 Loop is an integral test facility, the tests have to

provide insight into rapid boron-dilution transients in prototype plants.

The premise of the test is that an interfacing-system leak has caused the ingress of deborated water into the primary system. This nearly-stagnant deborated water has accumulated in one of the steam generators. The deborated slug is inadvertently set in motion by the actuation of one of the pumps connected to the steam generator in which the slug has accumulated. As it travels through the system, the deborated water at the front and end of the slug mixes with the borated primary coolant present in the system. By the time the slug reaches the core entrance, its boron concentration has increased due to the mixing. However, the boron concentration of the slug will vary both temporally and spatially. Whether or not a significant reactivity

excursion will result following the penetration of the slug into the core depends on the boron concentration of the fluid in both time and space. The initial/boundary conditions and geometry dependence of core-inlet boron-concentration has been recognized early in rapid boron-dilution investigations, and confirmed during the UM 2x4 Loop experimental program. To predict the potential consequences of different initiating scenarios in different reactors, simulations are desirable. The UM tests focus on the downcomer region which is where most of the re-boration of the slug occurs (Fig. 1). The preponderance of mixing is induced by turbulent eddies caused by either geometric discontinuities (including the pump impellers) or large velocity gradients among adjacent streams of fluid. The tests are designed to make a transition from a configuration that is nearly special effect to full integral test.

1.1 Test A—single inlet, single outlet, external tank injection

Approximately 20 tests were run with the boundary conditions given to participants (93% pump speed and approximately 60°C temperature difference between the primary coolant and the front). The temperature differences were measured with thermocouples. The tests show good repeatability. Initial investigations have shown that heat losses are below 10% over the duration of the transient (approximately 60 seconds). The primary system is initially well mixed at 74°C. The simulation boundary conditions consist of:

- slug flow rate as a function of time,
- temperature as a function of time at the inlet of the simulation boundary, and
- pressure drops in the core region.

Fig. 2 shows the temperature measured by the central (middle of downcomer) thermocouple as a function of time during the test. The other two functioning inlet thermocouples read within the instrument error of 1° C. The slug injection flow rate was determined from the level drop of the injection tank. Fig. 3 shows the injection flow rate time history.

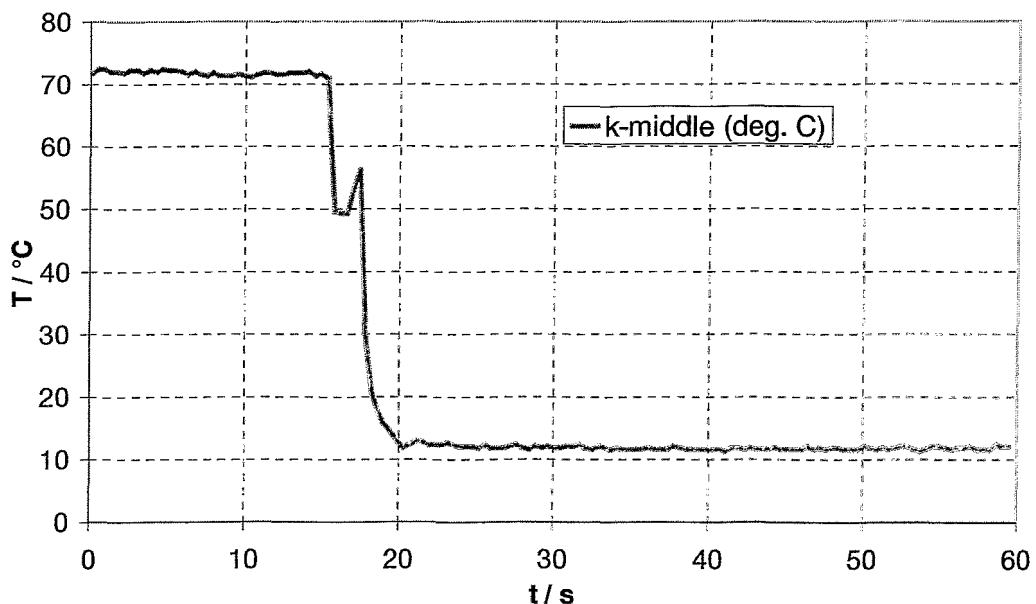


Fig. 2 Inlet temperature history for test A

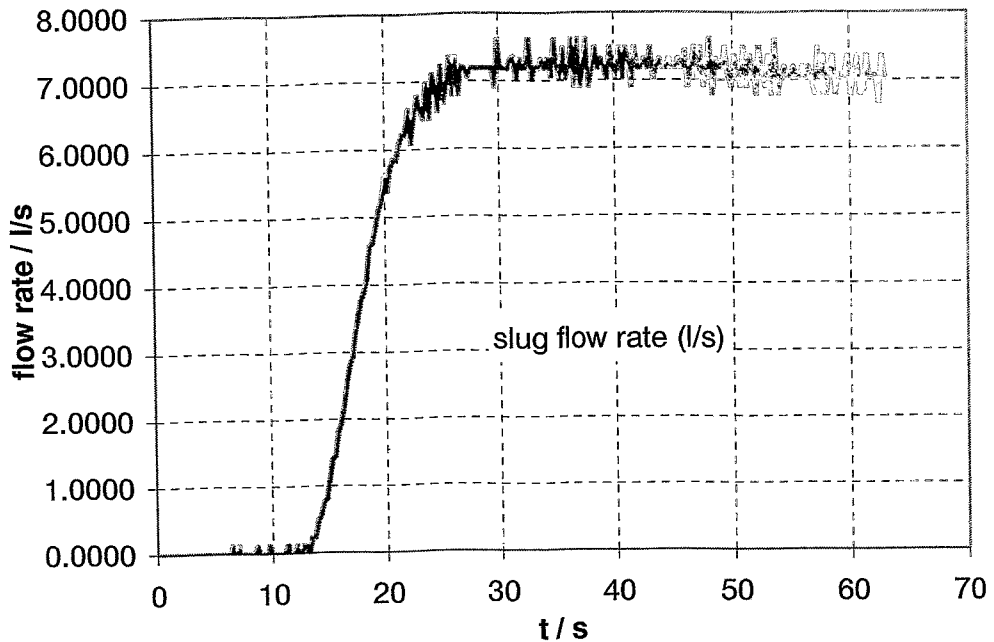


Fig. 3 Slug injection flow rate history for test A

1.2 Test B—single inlet, single outlet, steam generator injection

The Loop is operated as a closed system throughout this test series. The slug is placed at the bottom of SG A. When pump A1 is started, the slug proceeds through CL A1 (see Fig. 1) into the downcomer, up through the core and exits through HL A. All other cold legs are isolated. Initial investigations have shown that heat losses are below 20% over the duration of the transient (approximately 200 seconds). Four tests were run with the boundary conditions given to participants (93% pump speed and approximately 60°C temperature difference between the primary coolant and the front). The tests show great repeatability. The primary system is initially well mixed at 69°C. The simulation boundary conditions consist of:

- slug flow rate as a function of time,
- temperature as a function of time at the inlet of the simulation boundary, and
- pressure drops in the core region.

Fig. 4 shows the average temperature measured by the three working inlet thermocouples as a function of time during the test. The three inlet thermocouples read within the instrument error of 1° C. The flow rate was determined from the calibrated ultrasound flow meter. Fig. 5 shows the injection flow rate time history.

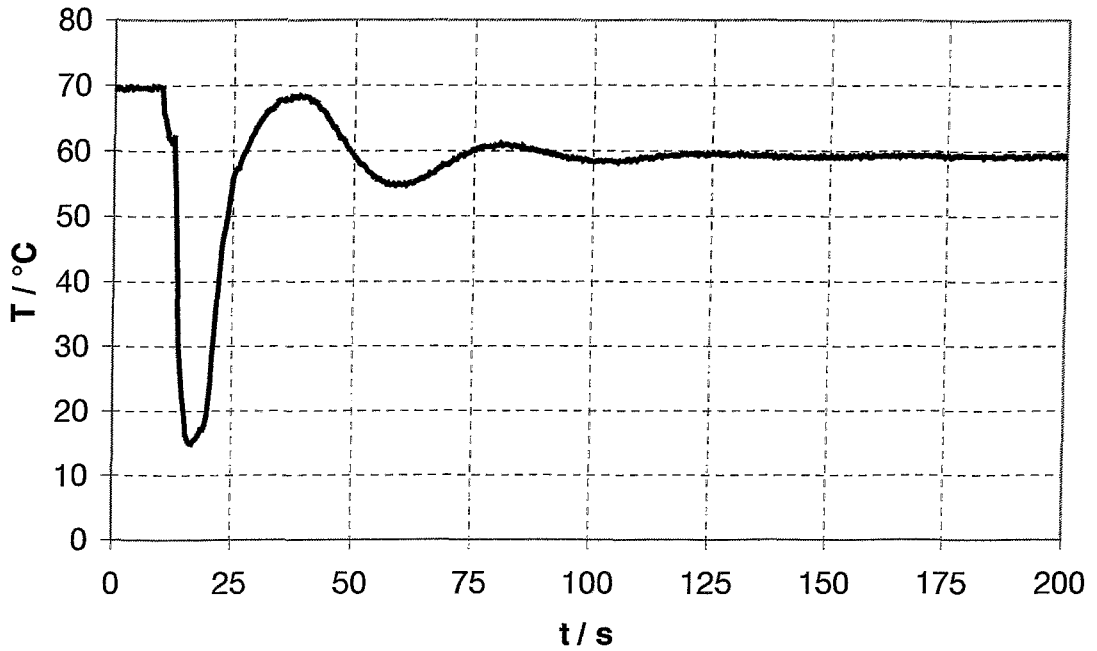


Fig. 4 Inlet temperature history for test B

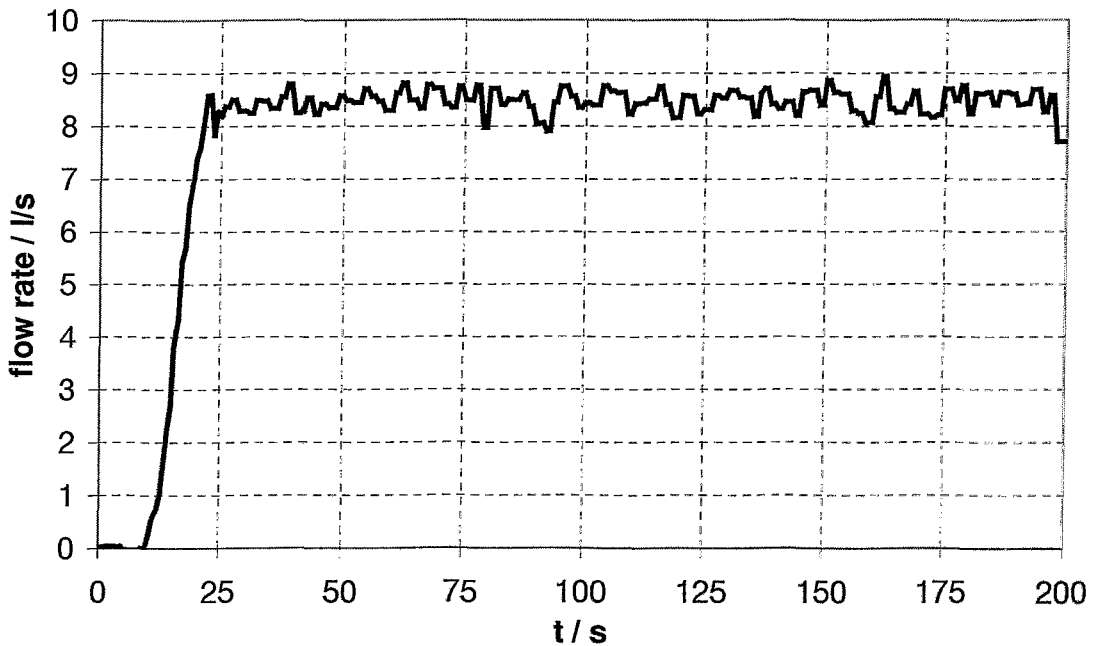


Fig. 5 Slug injection flow rate history for test B

2. Temperature Measurement

Previous experiments at UM and elsewhere have shown that the slug mixing occurs predominantly in the downcomer. To trace the temperature field there, altogether 286 TCs are mounted in the downcomer and the lower plenum of the reactor vessel on 11 horizontal planes

labeled Level 1 through Level 11. Level 1 denotes the lowest plane and Level 11 denotes the uppermost plane. The vertical location of all levels is measured from the axis of the cold leg nozzles and is given with positive numbers for levels below the cold leg nozzle axis and with positive numbers for levels above the reference point as shown in Fig. 6 below.

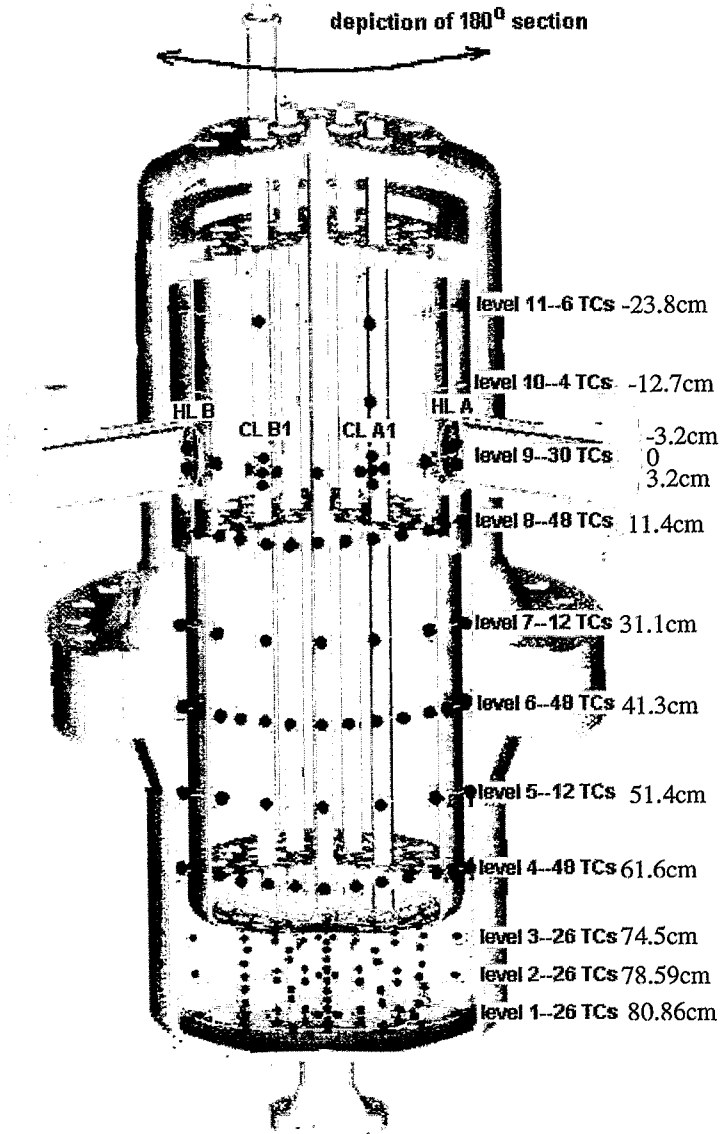


Fig. 6 Thermocouple levels in the reactor downcomer and lower plenum

Levels 1, 2, and 3 are located within the lower reactor plenum and each level contains 26 TCs. This makes 78 TCs for the whole volume of the lower plenum. For each level, the TCs are uniformly spaced along three concentric circles. There are 2 TCs on the innermost circle of 0.02 m radius, 12 TCs on the middle circle of 0.0825 m radius, and 12 TCs on the outer circle of 0.165 m radius. The center point of the circles is located on the axis of the reactor vessel. Level 1 is located 0.8721 m below the cold leg nozzle axis and Level 2 is placed 0.8086 m below the reference point. The TCs for Level 3 are 0.745 m below the cold leg nozzle axis with the exception of the two TCs on the innermost circle that are located 0.7859 m below the reference point. There is no azimuthal angle displacement between the TC locations for all three levels and a top view of the TC positions is shown in Fig. 7 below.

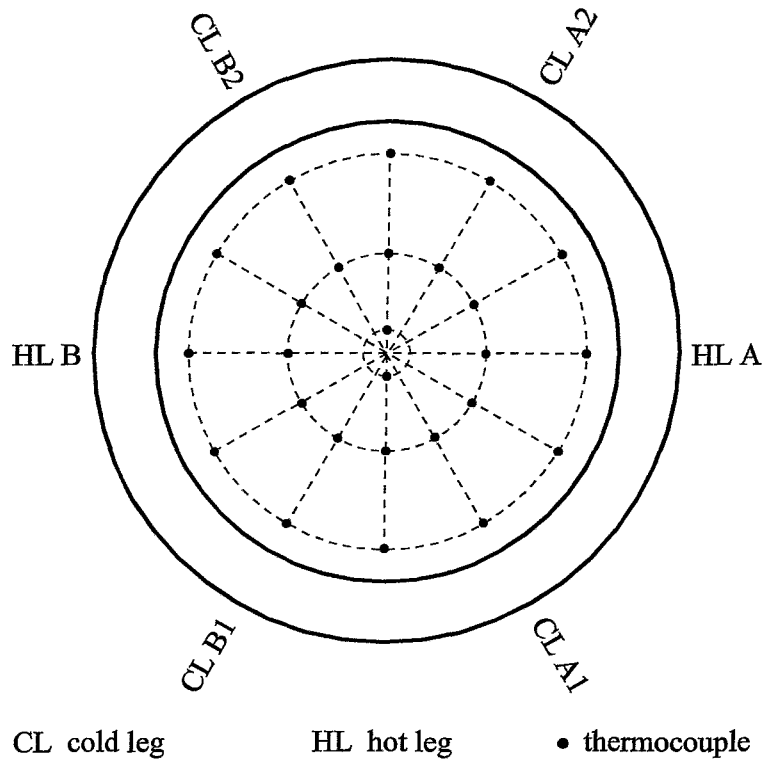


Fig. 7 Thermocouple positioning in the lower plenum (Levels 1, 2, and 3)

Levels 4, 5, 6, and 7 are located in the lower portion of the downcomer, which has a larger gap flow area. The TCs on Level 4 are located 0.616 m below the cold leg nozzle axis. This level is at the downcomer outlet and therefore is heavily instrumented. The TCs are located at an azimuthal angle increment of 15° at the middle of the annulus gap. At alternating azimuthal TC locations, the central TC is augmented by two more TCs located at different radial positions. The additional TCs are used to examine the radial variation of the slug temperature in the downcomer. The outer TC is located at a distance of 0.006 m from the vessel wall and the inner TC is at the same distance from the barrel wall. Thus, there are 12 inner TC, 24 TCs central TCs, and 12 outer TCs, which make 48 TCs altogether on this level. The TCs arrangement for Level 4 is illustrated in Fig. 8. Level 5 is located 0.514 m below the cold leg nozzle axis and contains 12 TCs located at the middle of the downcomer gap. The TCs are equally spaced along the downcomer perimeter. The arrangement for Level 5 is illustrated in Fig. 8. Level 6 is located 0.413 m below the cold leg nozzle axis and contains 48 TCs arranged as on Level 4. Level 7 is positioned 0.311 m below the cold leg nozzle axis and contains 12 TCs arranged as on Level 5. It is important to notice that Level 6 is located 7 expansion step heights downstream of the elevation of the expansion step and Level 7 is located 5 expansion step heights downstream the expansion step. This corresponds to the expected position for flow reattachment at 5 to 7 step heights downstream of the backward facing step.

Fig. 8 below illustrates the TC arrangement for Levels 6 and 7.

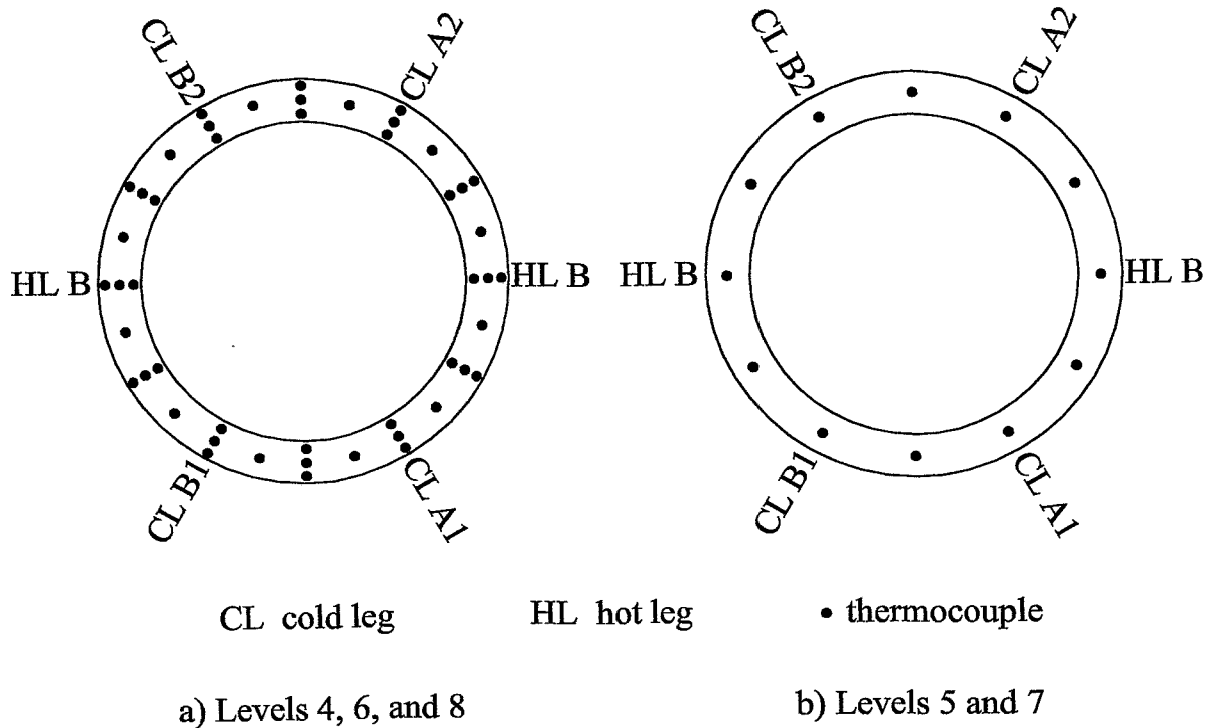


Fig. 8 Thermocouple positions in the downcomer (Levels 4, 5, 6, 7, and 8)

All other levels are located within the upper part of the reactor downcomer, which has a smaller gap flow area. Level 8 is located 0.114 m below the cold leg nozzle axis and has 48 TCs arranged as on Level 4 as shown in Fig. 9. Level 9 is at the height of the cold and hot leg nozzles and it contains 30 TCs. There are 5 TCs positioned at the interface of each cold leg nozzle with the downcomer outer wall. One TC is at the axis of the cold leg nozzle and the other 4 are positioned at a distance of 0.032 m from that axis along the cold leg nozzle vertical and horizontal diameter. In addition, 6 TCs on Level 9 are positioned in the downcomer between the adjacent leg nozzles at the middle of the gap. The last 4 TCs measure the temperature in the upper plenum at the inlet points to both hot leg nozzles. There are 2 TCs located at the inlet to each hot leg nozzle. Both TCs are positioned at a distance of 0.032 m from the hot leg axis along the vertical hot leg nozzle diameter. The distance between each of these TCs and the reactor vessel vertical axis is 0.241 m. The arrangement of Level 9 TCs is illustrated in Fig. 9. Levels 10 and 11 are located in the portion of the downcomer above the leg nozzles and they contain relatively few TCs. Level 10 is located 0.127 m above the leg nozzle axes and has 4 TCs. They are positioned at the middle of the downcomer gap at an azimuthal angle interval of 90°. Level 11 is located 0.238 m above the cold leg nozzle axes and contains 6 TCs, which are also positioned at the middle of the downcomer gap. These TCs are positioned at an azimuthal angle interval of 60°. Fig. 10 illustrates the positions of Level 10 and 11 TCs. Table 1 shows the positions of all thermocouples.

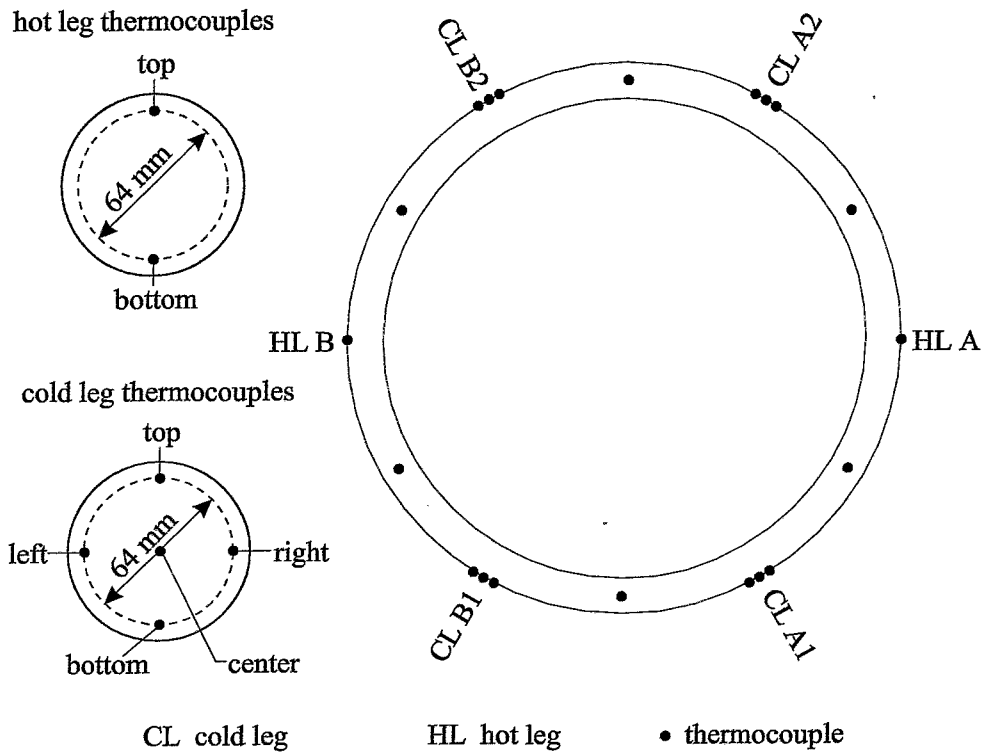


Fig. 9. Thermocouple positions in the downcomer nozzle area (Level 9)

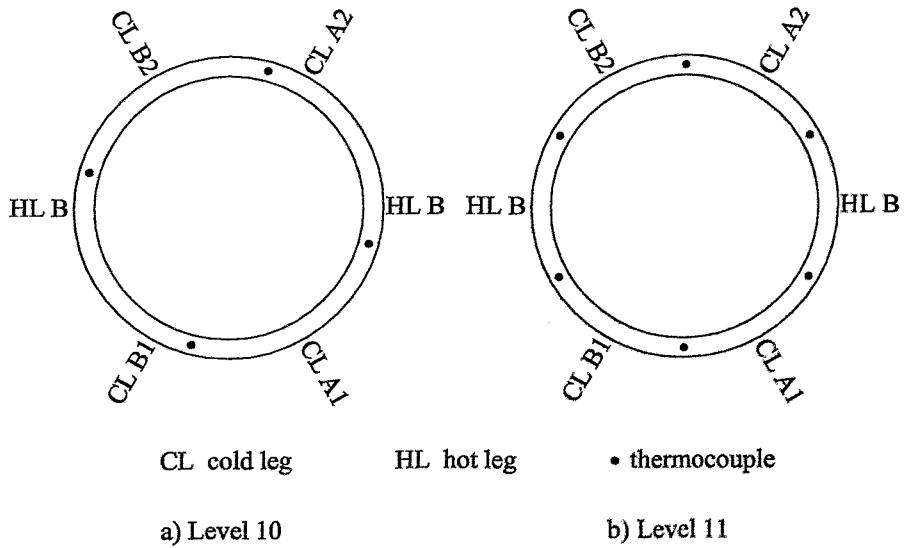


Fig. 10 Thermocouples in the downcomer above nozzle area (Levels 10 and 11)

Table 1 Thermocouple instrumentation in the 2x4 loop vessel

Vessel Region	Level	Elevation (m)	TC Number	TC Type
Downcomer above nozzles	11	-0.2380	6	T
	10	-0.1270	4	T
Nozzle area	9	-0.0320	6	K(20)/T(10)
		0	18	
		0.0320	6	
Above step	8	0.1140	48	T
Downcomer below step	7	0.3110	12	K
	6	0.4130	48	K
	5	0.5140	12	K
	4	0.6160	48	K
Lower plenum	3	0.7450	24	K(3)/T(23)
		0.7859	2	
	2	0.8086	26	K(25)/T (1)
	1	0.8721	26	K

3. Computational Modeling

The 3-D computational fluid dynamics (CFD) codes provide an effective tool for mixing calculations. In recent years, the rapid development of both the software and the computers has made it feasible to study the coolant mixing in sufficient detail and to perform the calculations for transient conditions.

The used CFD-Code for mixing studies at the Forschungszentrum Rossendorf (FZR) is CFX-4. CFX [CFX] is a finite volume program that offers the following options, which can be used in the mixing studies:

- Solution of the Navier-Stokes-Equations for steady and unsteady flows for compressible and not compressible fluids
- Applicability for laminar and turbulent flows (different turbulence models)
- Porous media model, implementation of body forces added to the momentum equation, user defined scalar fields

3.1 Choice of models and nodalization

3.1.1 Turbulence modeling

The modeling of the turbulence is important both for the flow field and the concentration field. At the same time turbulence modeling is one of the biggest problems in the field of the CFD. In the boron diluted slug mixing calculations made so far the mostly used turbulence model are the standard K- ϵ model and its variations like RNG K- ϵ model. Some occasional tests are made also with Reynolds Stress Model (RSM) and even using Large Eddy Simulation (LES) [Be]. However in spite of the well-known limitations the most common and the most robust models like k- ϵ seems to be most often used. In the calculated cases the

standard K- ϵ model was used. Calculation were also performed without any turbulence model (laminar).

3.1.2 Numerical diffusion, nodalization and time step size

Numerical error is a combination of many aspects; the grid density, discretization method, time step size and convergence error have all their own effect. When a validation of the computational model is made using a certain experiment, the separation of different numerical effects is difficult; for example, the numerical diffusion, i.e. a numerical error which acts like an artificial extra diffusion, can affect to the result in the same direction like too large turbulent viscosity used in some turbulence models.

The numerical diffusion can be minimized using denser grids, higher order discretization methods and suitable time step size. Often the computation time puts some limits for these, but anyhow in all CFD computations results should be ensured to be grid and time-step independent, and if not possible, the uncertainties should be quantified. If the time steps are too large the influence of numerical diffusion on the results is very high, if the time steps are too small the computational time exceeds.

Generally, it is important to find an optimum between acceptable results and computational time. In the calculated cases the optimum is a time step of 0.1 s.

3.2 *Model assumptions, geometry preparation and grid generation*

An incompressible fluid was assumed for the coolant flow in pressurized water reactors.

The inlet boundary conditions (velocity, temperature, etc.) were set at the inlet nozzles. The outlet boundary conditions were pressure controlled. Passive scalar fields as well as temperature differences according to the given boundary conditions were used to describe the boron dilution processes.

The calculations were done on a SGI Origin 200 (1 GB RAM, 4x R 10000 180 MHz, 64 Bit CPU) workstation platform. The generated grid contained ca. 450000 nodes. The transient calculations last a few weeks.

The nodalization (grid generation) of the reactor pressure vessel (RPV) was carried out step by step (Fig. 11). This allowed to analyze the influence of geometric details on the flow. The following important factors were identified: Exact representation of the inlet region (bend radii etc.), extension of the downcomer below the inlet region and obstruction of the flow by the outlet nozzles cut through the downcomer. The Internals have a strong influence on the flow field and therefore on the mixing. The core support plate and the core are modeled as a porous region (Fig. 12). The porosity value γ for perforated plates is determined by relating the area of orifices to the total area of the sieve. Body forces B are added to the momentum equation, to take into account distributed friction losses in the sieve plate and the core. In the model, only the second order contribution of the body forces is used being typical for turbulent flow. The corresponding coefficient is obtained from calculated values for the flow resistance coefficient.

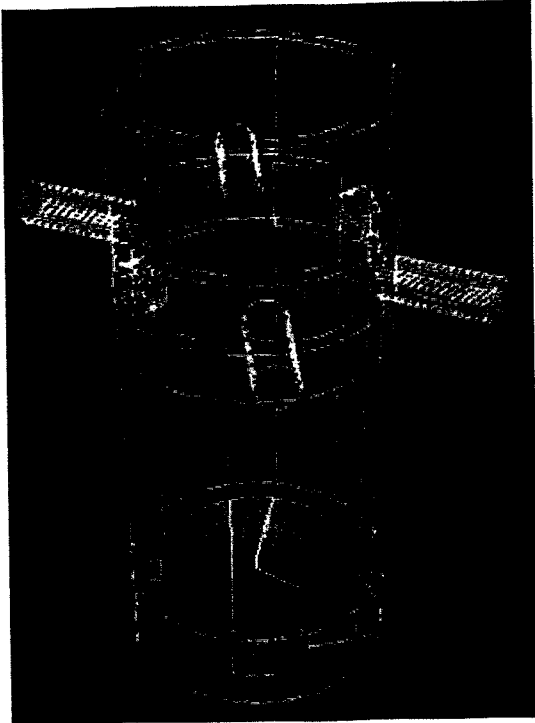


Fig. 11 Grid model with core support

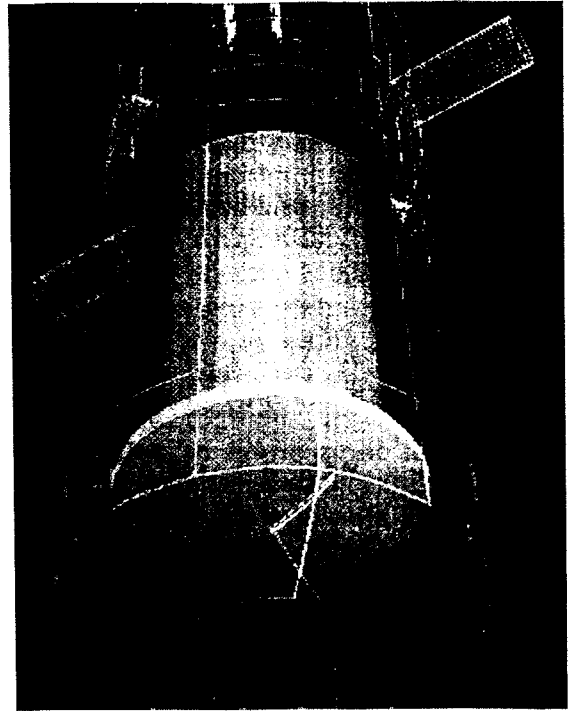


Fig. 12 Core support plate and core

According to the positions of the thermocouples a user subroutine in the CFX flow solver was written to extract the needed data from the calculated flow and temperature field to compare it with measured data.

4. Results

4.1 Test A

Fig. 13 shows streamlines representing the transient velocity field in the downcomer and lower plenum (including the lower support plate) at the pump start-up scenario of Test A calculated with CFX-4.3. The corresponding start up ramp of the experiment is printed in Fig. 3. The flow field is nearly constant after 30 s.

Due to a pulse driven flow at the inlet nozzle the main flow in the downcomer is distributed into two main jets, the so called butterfly distribution. In addition several secondary flows are seen in various parts of the downcomer. Especially strong vortices occur in the lower plenum area on the left and right position of the injection loop. Here recirculation areas occur, which are controlling the size of other small swirls. The complex flow field promotes a good mixing of the front in the downcomer.

The qualitative results of a pump start-up simulation are shown in Fig. 14. Although the front divides into several parts a main front layer propagates towards the core on the left and right side of the injection loop. Afterwards the front is distributed over the core support plate (Fig. 14).

A comparison of the experimental data with the numerical simulation in a few selected thermocouple positions are shown in Fig. 15. Calculations were made with and without modeling buoyancy effects. The differences between the temperature profiles of this calculations are small, so it seems buoyancy is not the dominating force. The largest differences between these calculations show the diagram at level 7. In the calculations taking into account buoyancy the front of lower temperature reaches these positions earlier. The comparison between calculation and experimental data at different levels shows, that primary temperature decrease is in good agreement with the measured data. However, the temperature fluctuations at the thermocouples seconds after the first temperature decrease can not be modeled well. Temporary temperature increases are also observed at most of the measurement positions in the calculations (level 5-8, 4-8, 6-18).

In Fig. 16 the averaged data of selected thermocouple level are printed against the maxima, minima and averaged measured data. The global flow and mixing phenomena, like the two swirls at the left and right position of the injection loop in the lower plenum and the time dependent local position of the front are well modeled with CFX. All results of the CFX calculations at different levels are within the tolerance of the measurements.

A azimuthal plot of the temperature distribution in the unwrapped downcomer at level 4 and 8 is shown in Fig. 17. The general temperature distribution calculated with CFX in the downcomer at this levels at different times is in good agreement with the experimental data. This figure shows the two front layer propagating towards the lower plenum. At the opposite side of the starting loop after 23 s still coolant with ambient temperature remains. After 50 s the entire downcomer is filled with coolant with lower temperature.

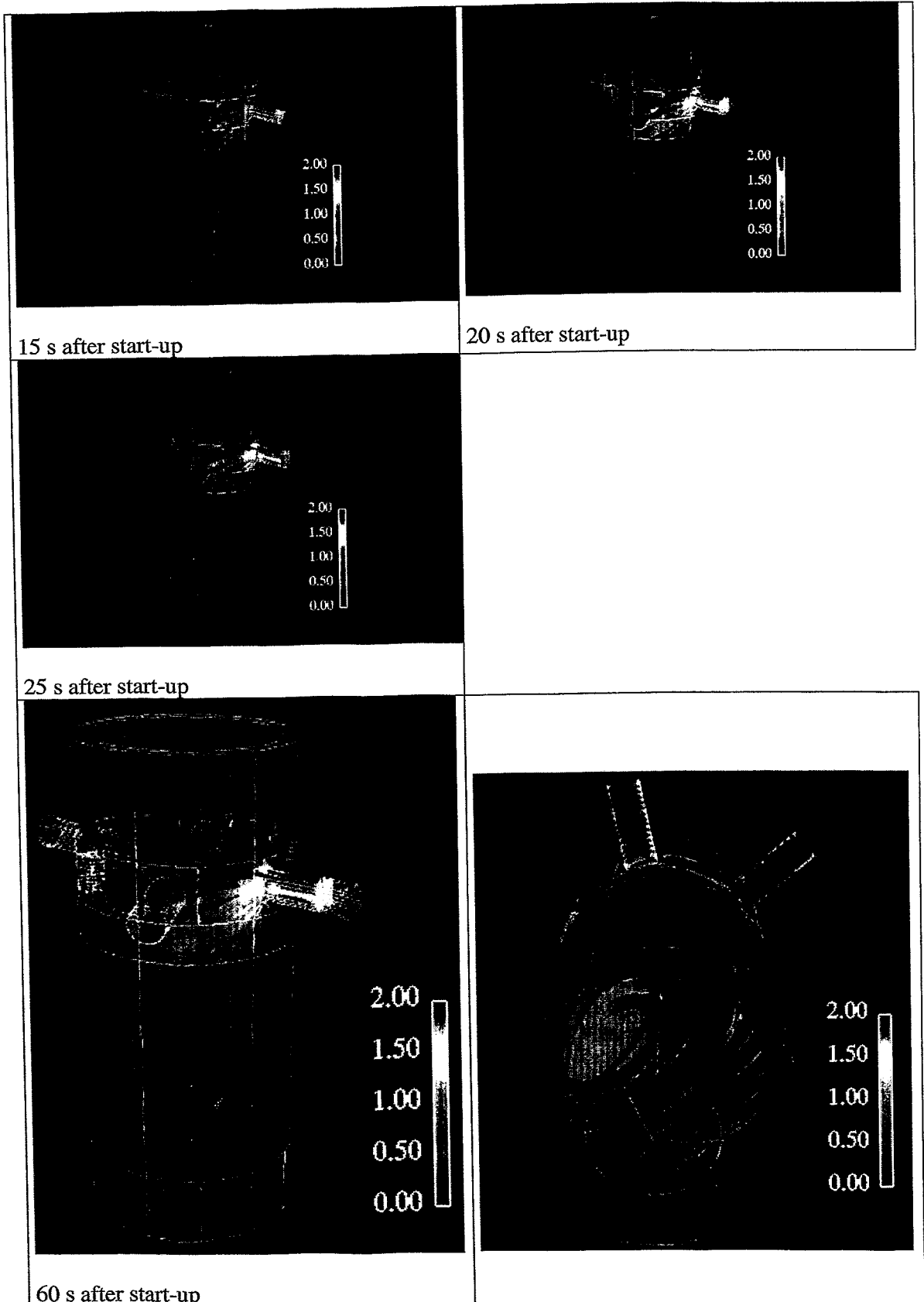


Fig. 13 Transient flow conditions at Test A (velocity)

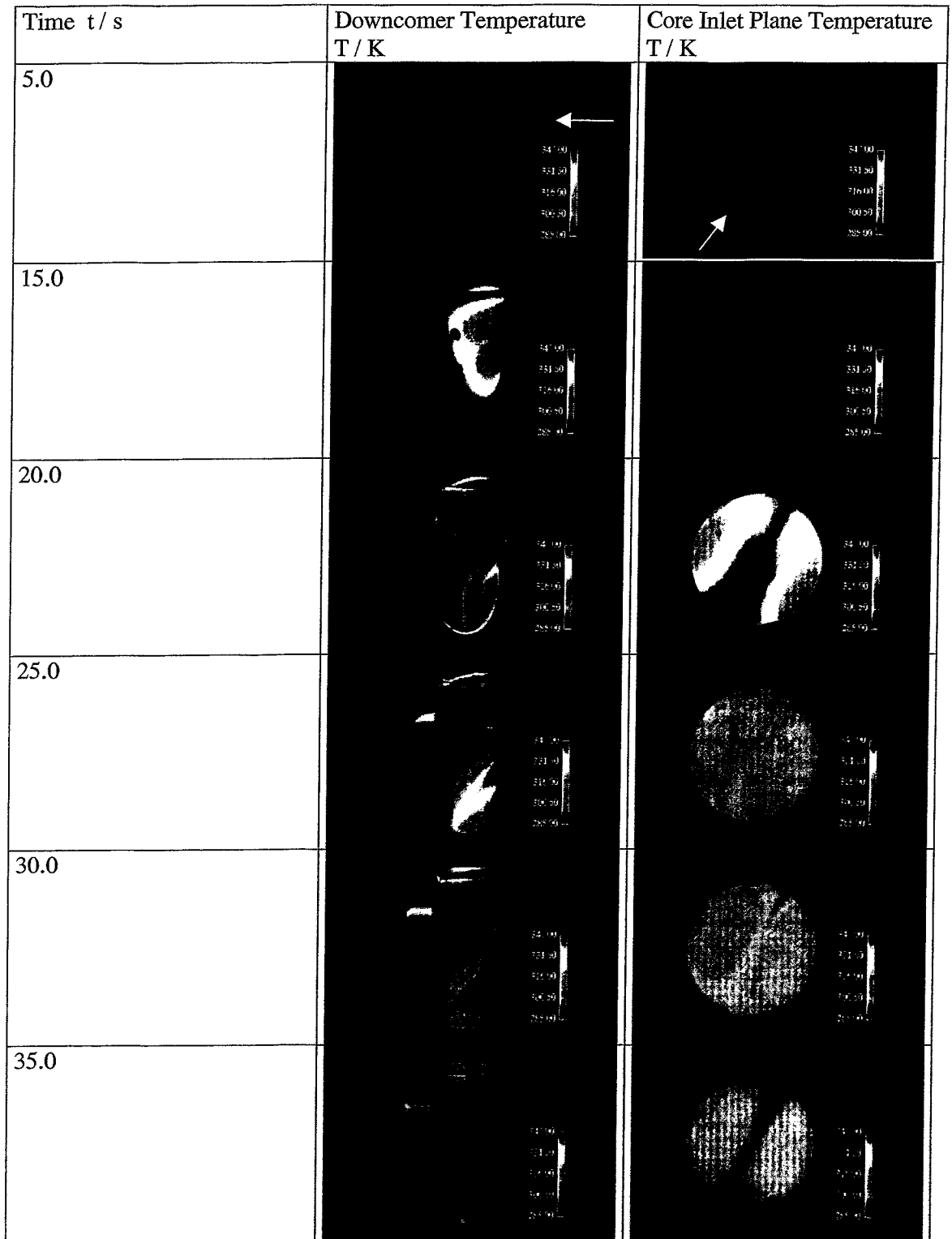
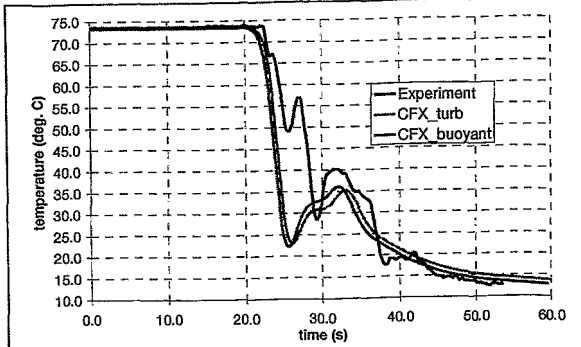
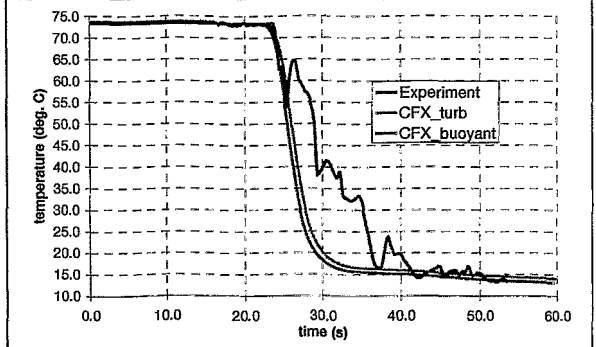


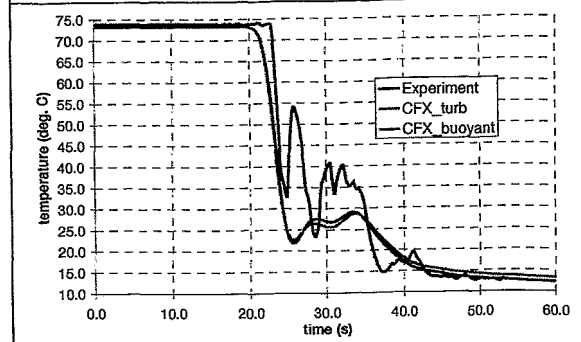
Fig 14 Time dependent mixing conditions at Test A, CFX



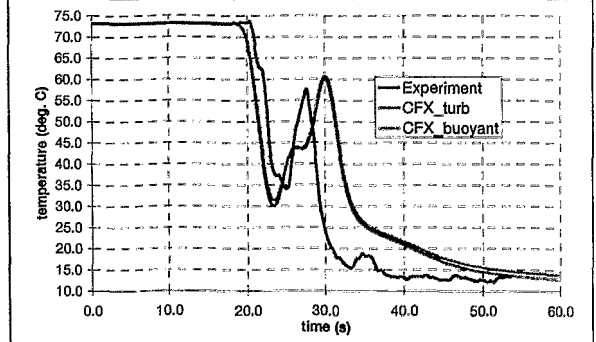
level 4-8



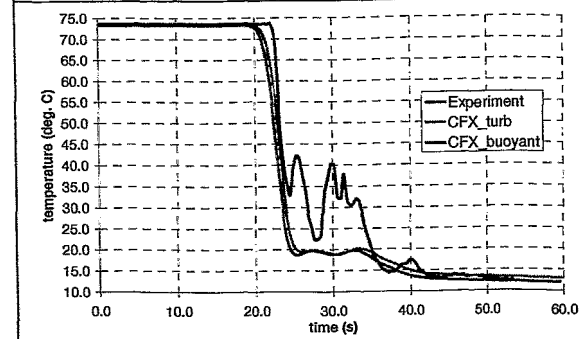
level 4-10



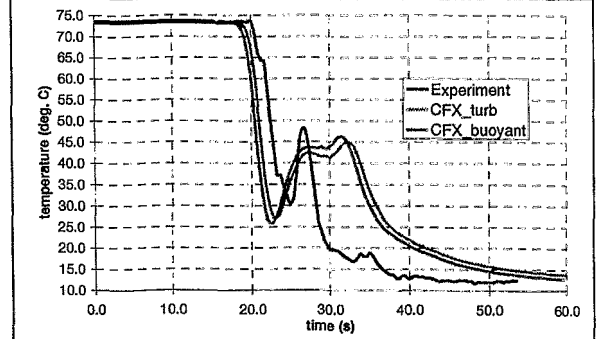
level 5-4



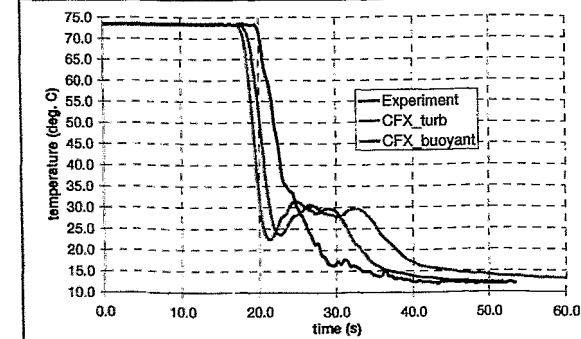
level 5-8



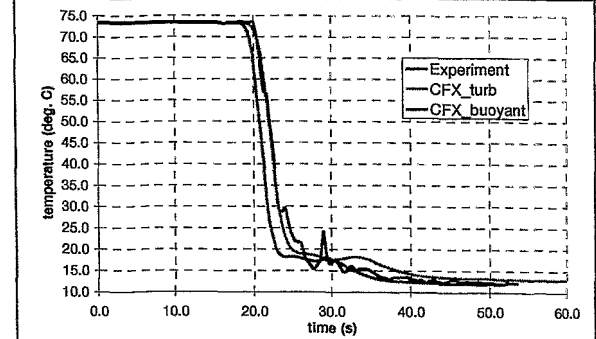
level 6-8



level 6-18



level 7-3



level 7-4

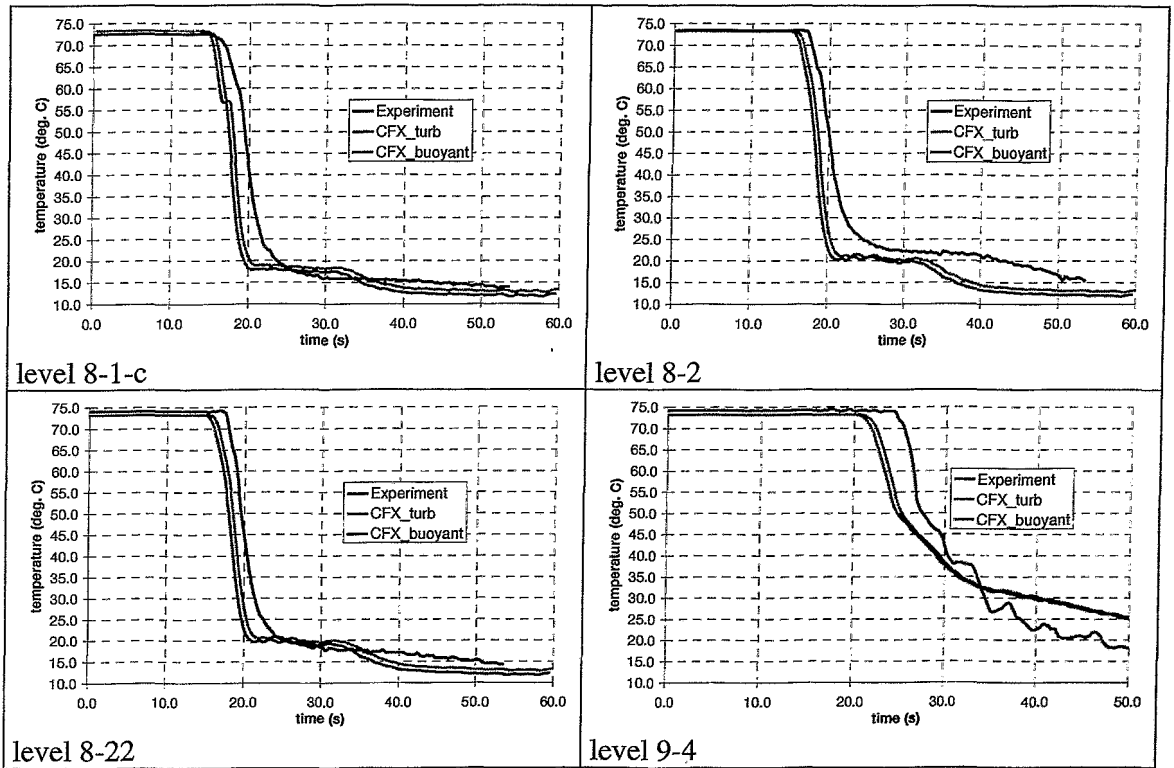


Fig. 15 Comparison Test A-CFX thermocouple positions

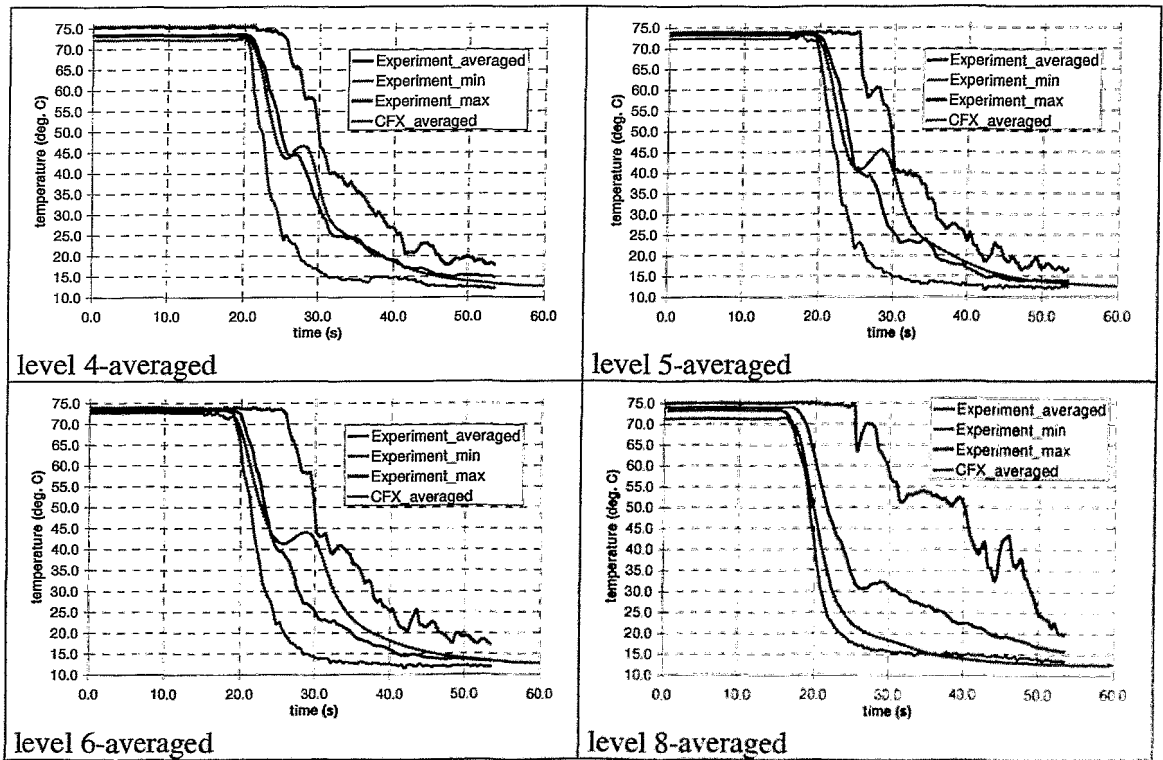


Fig. 16 Comparison Test A-CFX levels averaged

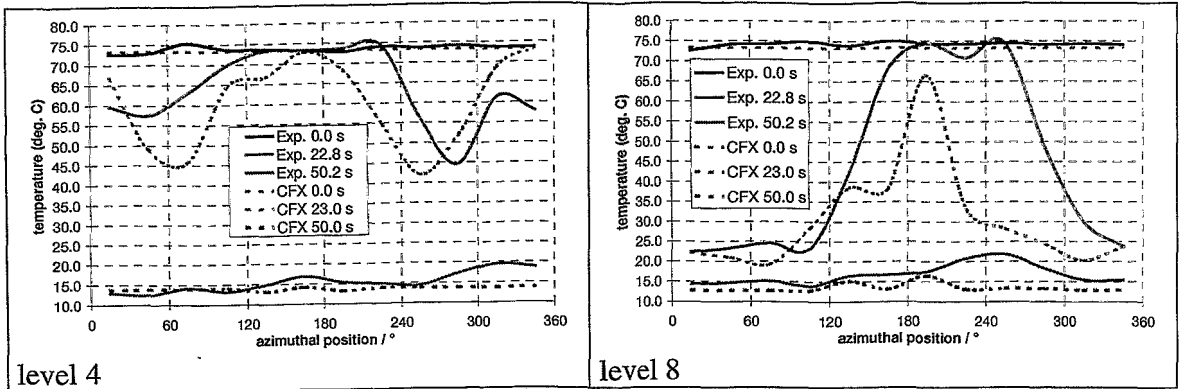


Fig. 17 Comparison Test A-CFX azimuthal positions

4.2 Test B

Fig. 18 shows streamlines representing the transient velocity field in the downcomer and lower plenum (including the lower support plate) at the pump start-up scenario of Test B at different times. The corresponding start-up ramp of the experiment is printed in Fig. 5. The flow field is nearly constant after 25 s. Although the start-up ramp is different to the ramp at Test A similar flow pictures occur. The main flow in the downcomer is also distributed into two main jets. Strong vortices occur in the lower plenum area as well on the left and right position of the injection loop. The qualitative results of a pump start-up simulation are shown in Fig. 19. Because of a slug formation as an inlet boundary condition compared to Test A different transient temperature distributions in the downcomer and at the core support plate occur. The slug enters the plate at left and right positions of the injection loop and is well mixed and distributed over the core support plate (Fig. 19).

A comparison of the experimental data with the numerical simulation in a few selected thermocouple positions are shown in Fig. 20. The CFX calculations were also made with and without modeling buoyancy effects. The differences between the temperature profiles of this calculations are getting bigger during the transient. After 60 s temperature differences of 5 K occur at some thermocouple positions. The comparison between calculation and experimental data at different levels shows a good agreement with the measured data at level 8 and 9, at the positions 4-9-c, 6-7-c, 6-19-c, and a poor agreement at the positions 4-1-c and 6-3-c.

In Fig. 21 the averaged calculated data of selected thermocouple level are printed against the maxima, minima and averaged measured data. The agreement between the calculations and the measured data is good. The global phenomena are again well modeled with CFX. All results of the CFX calculations at different levels are within the tolerance of the measurements.

A azimuthal plot of the temperature distribution in the unwrapped downcomer of level 4 and 8 is shown in Fig. 22. The agreement between azimuthal CFX and experimental data is less accurate than in the Test A. This is a result of a more complex transient mixing field compared to Test A, where only a front is propagating towards the core. The general temperature distribution calculated with CFX in the downcomer at this levels at different times is in the same range compared to the experimental data. After 50 s the entire downcomer is filled with coolant with medium temperature.

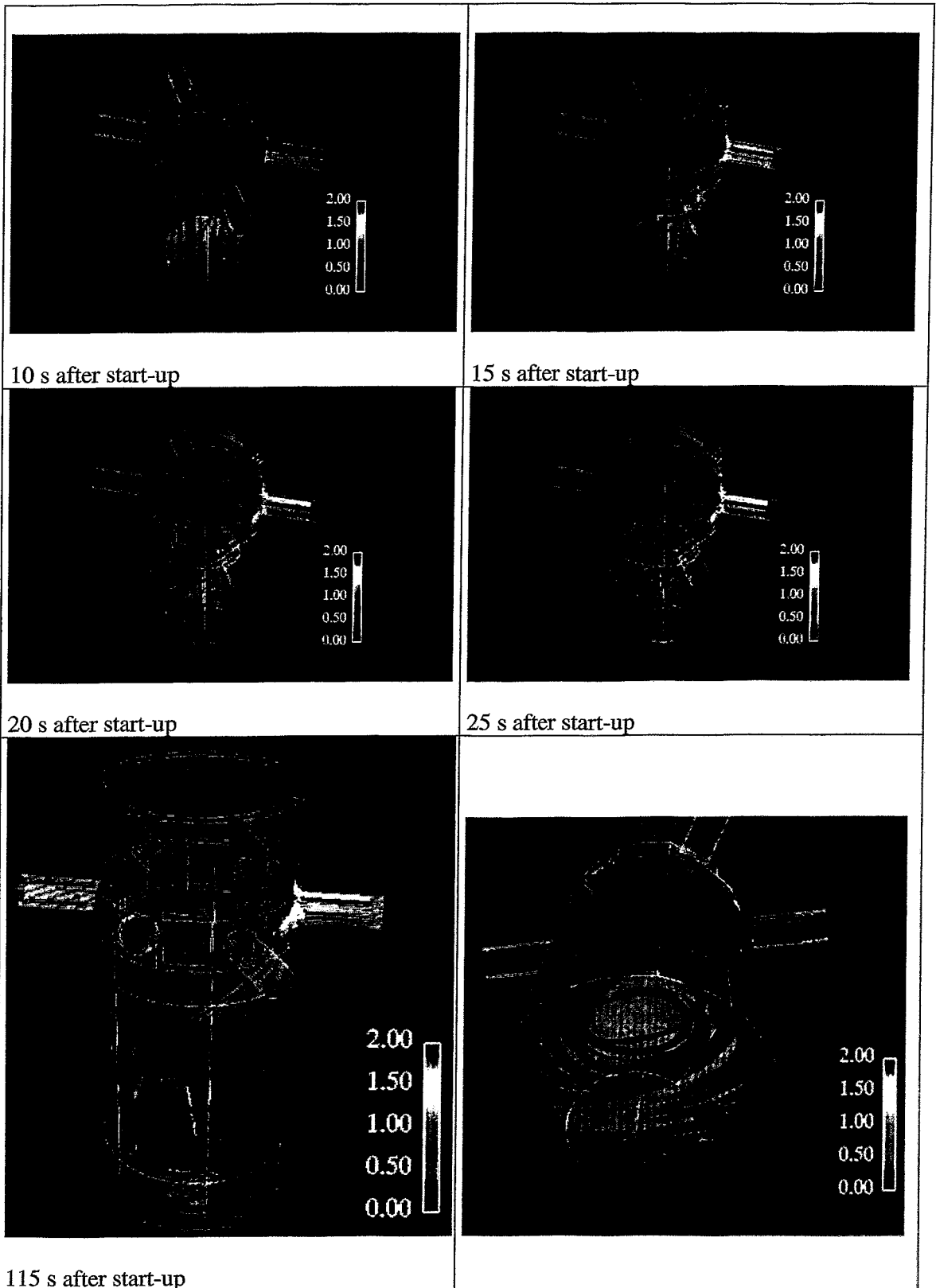
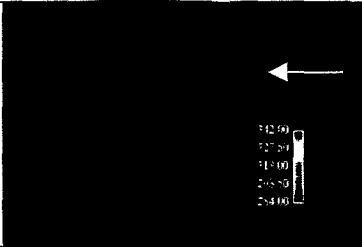
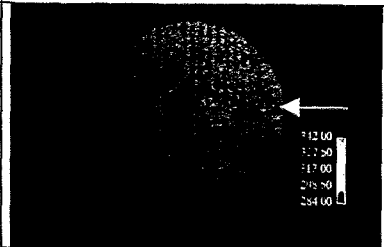
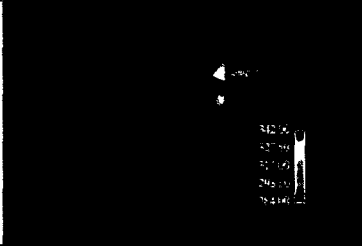
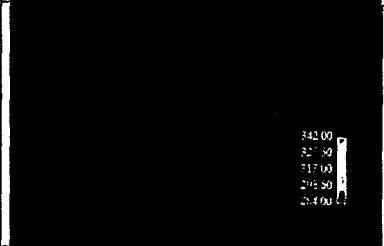
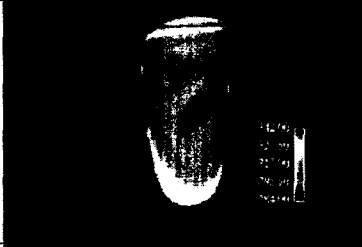
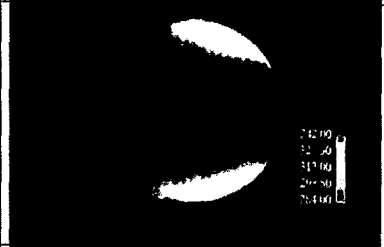
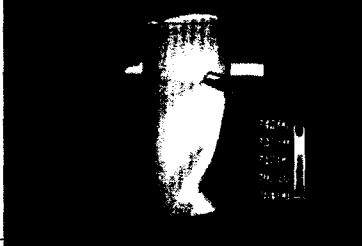
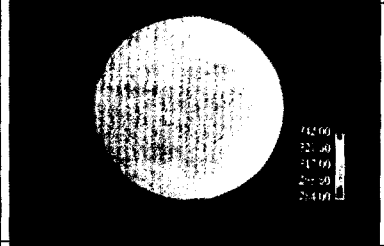
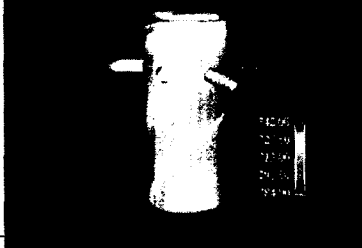
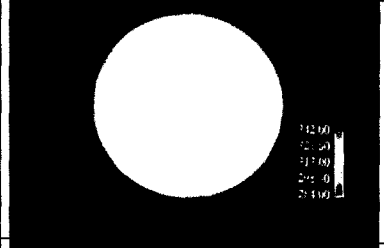
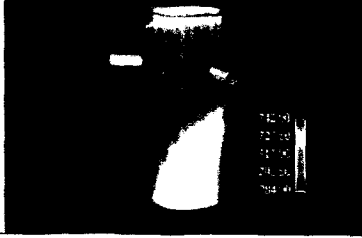
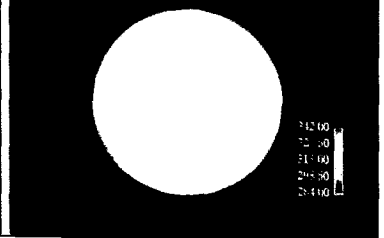
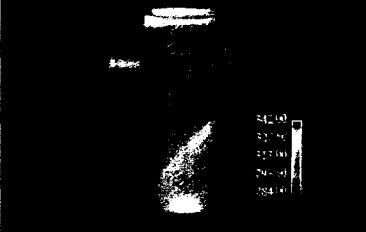
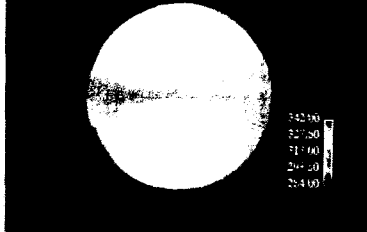
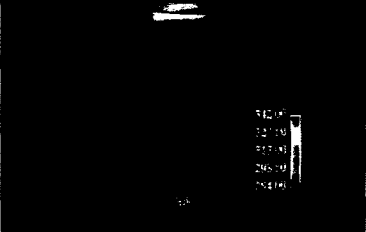
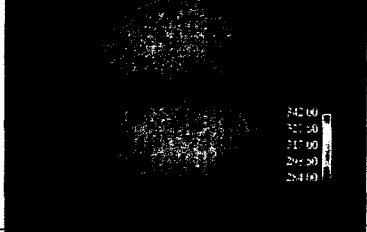

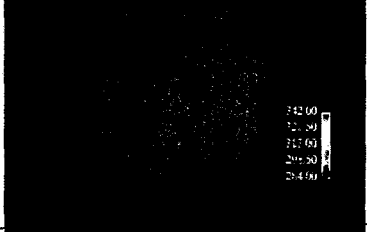
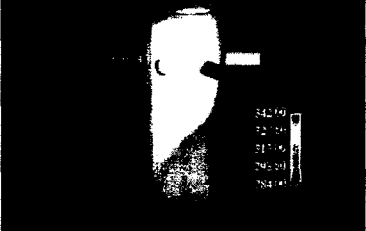
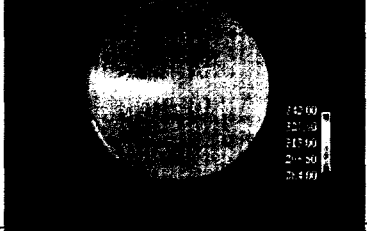
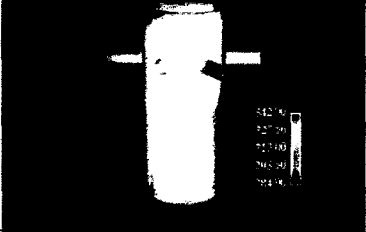
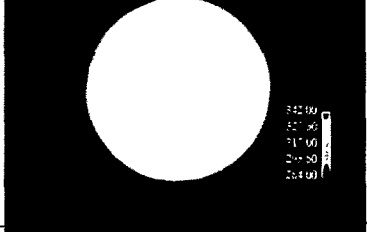
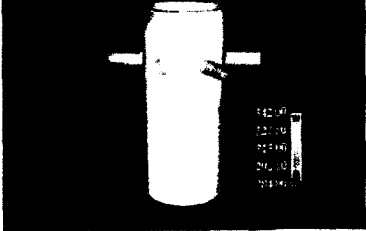
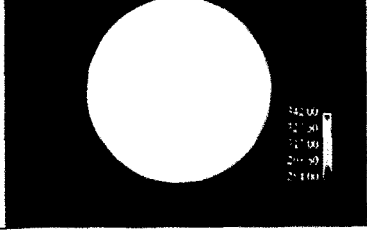


Fig. 18 Transient flow conditions at Test B

Time t/s	Downcomer Temperature T / K	Core Inlet Plane Temperature T / K
5.0		
10.0		
15.0		
20.0		
25.0		
30.0		

Time t / s	Downcomer Temperature T / K	Core Inlet Plane Temperature T / K
35.0		
40.0		
45.0		
50.0		
55.0		
65.0		

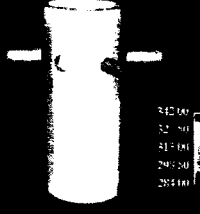
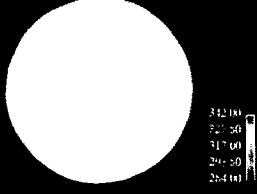
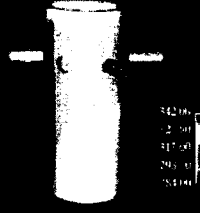
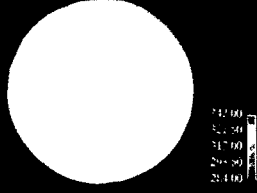
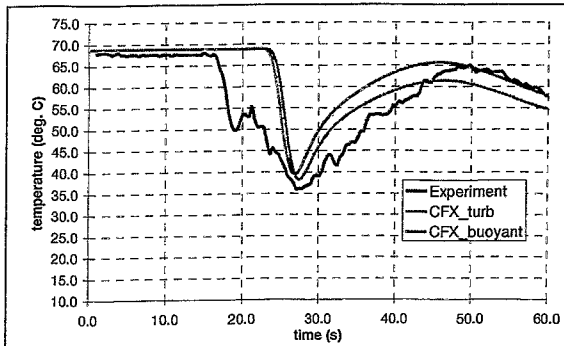
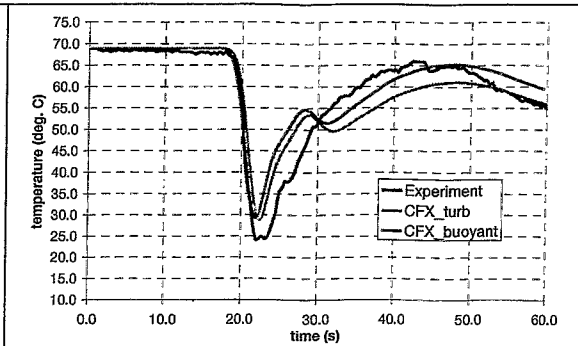
Time t / s	Downcomer Temperature T / K	Core Inlet Plane Temperature T / K
70.0	 <p>Temperature profile in the downcomer at 70.0s. The profile shows a vertical column with a temperature gradient from top to bottom. The values are: 342.00, 327.50, 313.00, 298.50, 284.00.</p>	 <p>Temperature profile at the core inlet plane at 70.0s. The profile shows a circular cross-section with a temperature gradient from center to periphery. The values are: 342.00, 327.50, 313.00, 298.50, 284.00.</p>
75.0	 <p>Temperature profile in the downcomer at 75.0s. The profile shows a vertical column with a temperature gradient from top to bottom. The values are: 342.00, 327.50, 313.00, 298.50, 284.00.</p>	 <p>Temperature profile at the core inlet plane at 75.0s. The profile shows a circular cross-section with a temperature gradient from center to periphery. The values are: 342.00, 327.50, 313.00, 298.50, 284.00.</p>

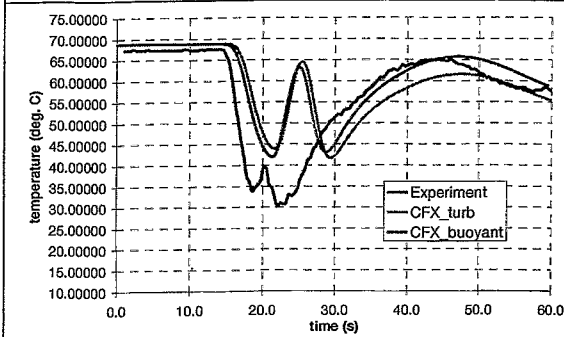
Fig. 19 Time depend mixing conditions at Test B, CFX



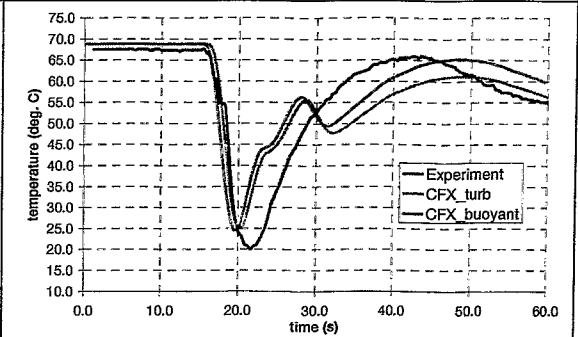
level 4-1-c



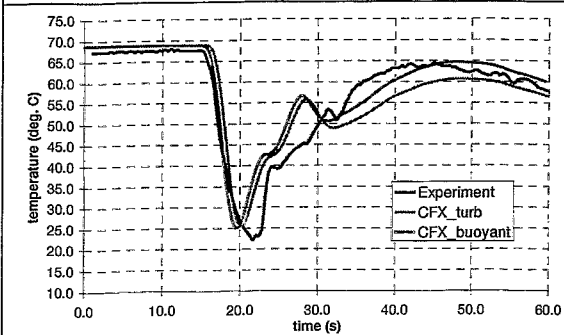
level 4-9-c



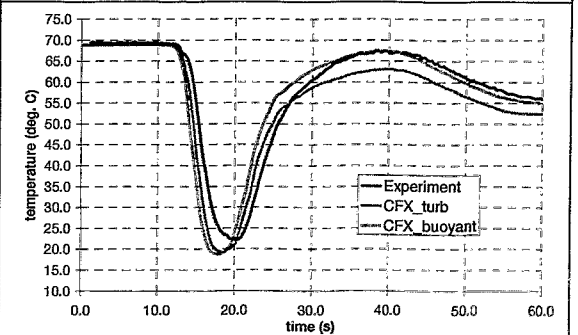
level 6-3-c



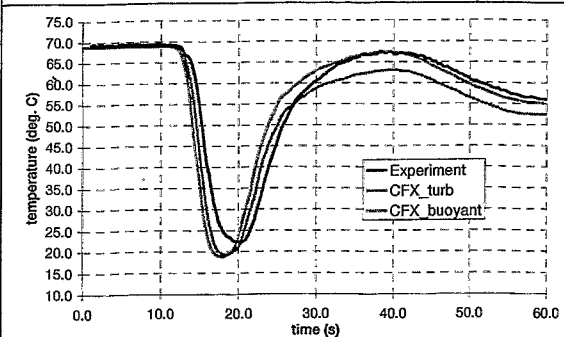
level 6-7-c



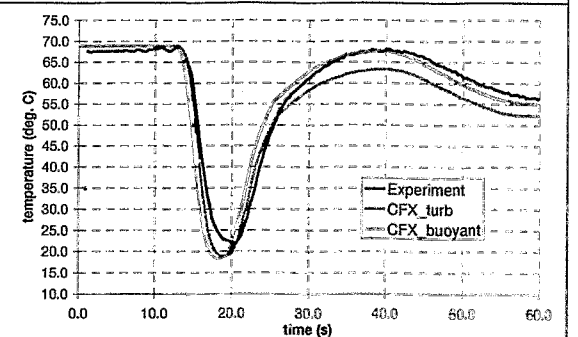
level 6-19-c



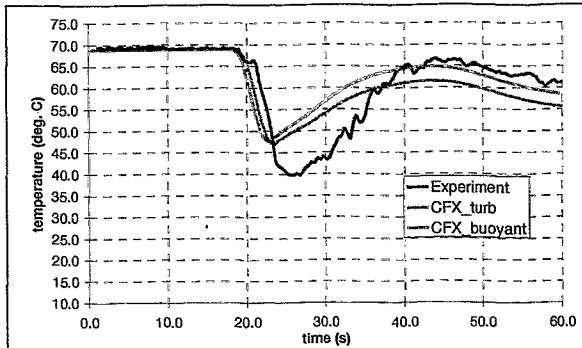
level 8-1-c



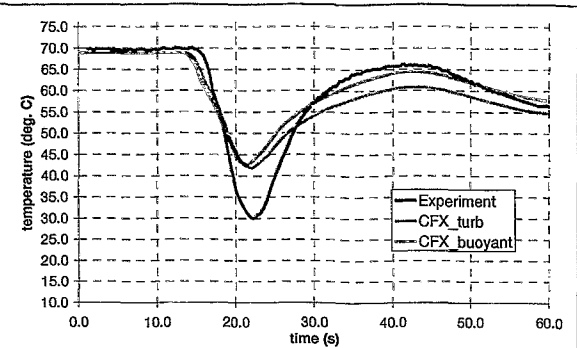
level 8-3-c



level 8-22

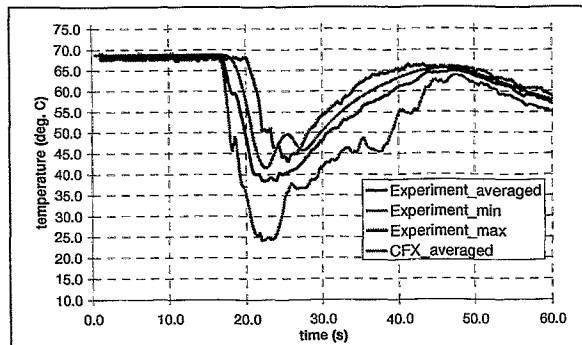


level 9-6

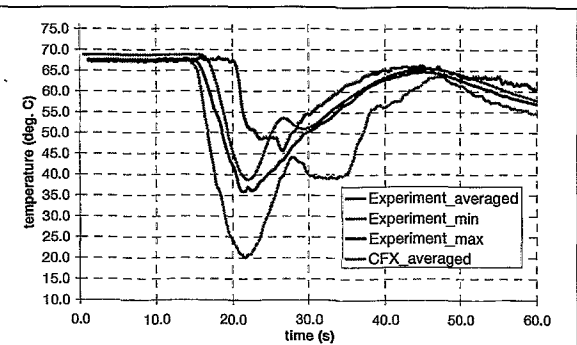


level 9-10

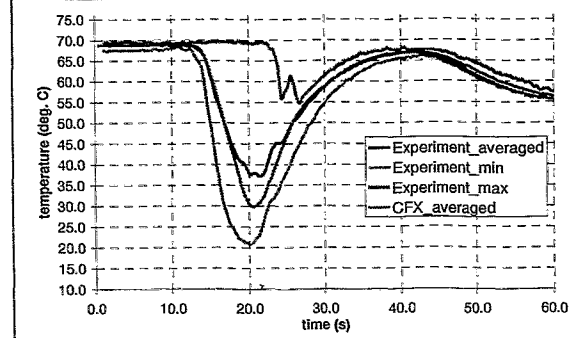
Fig. 20 Comparison Test B-CFX thermocouple positions



level 4-averaged

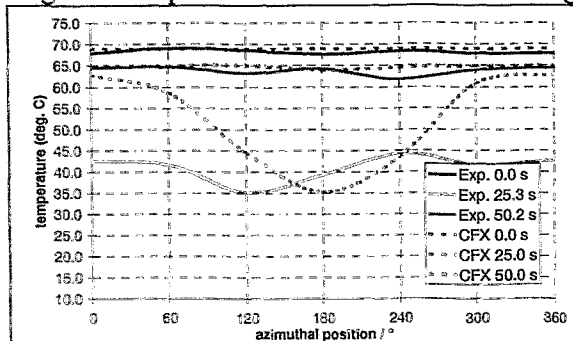


level 6-averaged

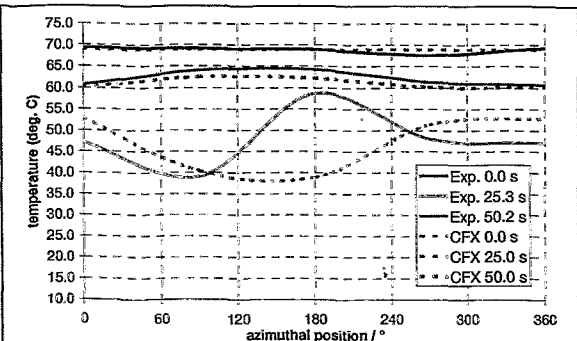


level 8-averaged

Fig. 21 Comparison Test B-CFX levels averaged



level 4



level 8

Fig. 22 Comparison Test B-CFX azimuthal positions

5. Conclusion

The need of the experimental support for validation of the computational tools to be applied to analyze the mixing of diluted slugs has been recognized in various countries. The test series for the International Standard Problem ISP-43 provides a platform for experiences to be applied to the simulation of a well-defined test series. Test A and B of the UM2x4 loop test facility were calculated with the CFD Code CFX-4.3. The results show qualitatively good agreement with the experimental data for both tests. The structure of the flow field and the form of the propagating temperature perturbation front are well modeled by the CFD code. However, deviations occur at local positions. Comparative calculations with and without taking into account buoyancy have shown, that buoyancy effects are noticeable, but the mixing is mainly momentum controlled.

Literature

- [Be] Bernard, J.P., Haapalehto, T., Review of Turbulence Modeling for Numerical Simulation of Nuclear Reactor Thermal-Hydraulics, Research Report, Lappeenranta University of Technology, 1996
- [CFX] CFX-4.4 User Manual (2001), AEA Technology
- [Ga] Gavrilas, M., Boron Mixing Code Assessment Test at the UMCP 2x4 Loop, 25th Water Reactor Safety Meeting, Oct. 22, 1997